

# Chapter 6

## THE EFFECTS OF NONDAMAGING LEVELS OF LASER ENERGY ON VISION AND VISUAL FUNCTION

JAMES W. NESS, PhD,\* AND JONATHAN M. NESS, BS<sup>†</sup>

---

### INTRODUCTION

#### ENTOPTIC LIGHT-LIMITING RESPONSES

##### Photic Blink Reflex

##### Spot Size to Intensity Relationship in Photic Blink Reflex

##### Pupillary Responses, Partial and Monocular Lid Closure, and Eye Movement

##### Effects on the Resolving Power of the Eye

#### MODELING INTRAOCULAR SCATTER

#### SCATTER MODEL VALIDATION

##### Blaser Visual Pursuit System

##### Photoreceptor Bleaching and Performance

##### Light-Limiting Strategies Revealed in Patterns of Afterimages

##### Pupillary Response and Performance

##### Assessment of Performance and the Entoptic Scatter Model

### CONCLUSION

\*Colonel, Medical Services Corps, US Army; Professor of Discipline, Photonics Research Center, US Military Academy, 601 Cullum Road, West Point, New York 10996

<sup>†</sup>Chemical Engineer, Argos, Summerville, South Carolina 29486

## INTRODUCTION

In 2014, Colonel James W. Ness (chapter author) received a call from a colleague in Afghanistan who was concerned about a “retinal laceration” diagnosis his driver received subsequent to a laser exposure at a checkpoint in the vicinity of Kabul. During the lead-up to the Afghan national elections, tensions were palpable. Checkpoints had been established randomly throughout Kabul. Nevertheless, “blue” (US and North Atlantic Treaty Organization [NATO]) convoys had been instructed to move rapidly around Kabul to avoid the placement of magnetic bombs on their vehicles while in traffic. Returning from an evening meeting between military commanders and local officials at about 19:30 local time, the colleague’s three-vehicle movement approached a random but poorly marked checkpoint. Seeing the convoy swerving around the checkpoint, the Afghan guard, following the rules of escalation of engagement, illuminated the lead driver’s windshield with a green laser at a distance of about 15 to 10 meters and closing. The driver’s left eye was exposed, and the driver reported feeling a sudden pain and something like a “snap” sensation. Unable to see and extremely disoriented, the driver immediately pulled over and swapped seats with his troop commander, who had occupied the front seat. The convoy then moved to the nearest forward operating base with an aid station. Care at an aid station includes triage, treatment, and evacuation, with care provided by a physician or physician assistant. There are no ophthalmic assets at this level of care.

While on the phone, Colonel Ness asked the colleague to detail the parameters of his driver’s exposure, from which retinal dose could be estimated and escalating concerns about the perceived hazard could be addressed. Given the initial “retinal laceration” diagnosis, the driver’s complaint of eyes watering for 2 days after exposure, and the need to keep one eye covered for 24 hours to mitigate light sensitivity symptoms, Colonel Ness advised his colleague that the driver should have a fundus exam. A trip to Bagram Air Base was encouraged.

In the meantime, Colonel Ness collaborated with a colleague from the laser safety community to estimate retinal dose based on the exposure information he gathered from his colleague in Afghanistan reporting the incident. Given the reported parameters and known official issue of laser interdiction systems to NATO forces, the laser source was assumed to be a B.E. Meyers Green Laser Interdiction System (GLIS), commonly used at checkpoints.<sup>1</sup> At the high setting, the GLIS has an output power of 200 mW at 532 nm with a beam divergence of 7 mrad. With the reported

ambient light conditions, a pupil diameter of 3.5 mm was estimated. The report of the incident also stated that the beam was scanned across the vehicle’s windshield, so the exposure duration chosen was 0.1 second.

Excluding the “dirty windshield” at 10 m from the source, the total intraocular energy (TIE) was estimated to be 0.5 mJ, or a total intraocular power of 5 mW, corresponding to a radiant exposure of 5 mJ/cm<sup>2</sup> at the cornea. The maximum permissible exposure (MPE) for a  $t = 0.1$  s exposure, given by the formula  $1.8 t^{0.75}$ , is 0.32 mJ/cm<sup>2</sup> at the cornea.<sup>2</sup> Visual disruption and likelihood of injury are estimated as follows: a glare effect is expected out to about 68 m from the source, the nominal ocular hazard distance (NOHD) is 14 m from the source, and there is a 50% chance of retinal damage ( $ED_{50}$ ) at a distance of 5 m from the source (see Chapter 9, Laser-Induced Ocular Effects in the Retinal Hazard Region, this volume).<sup>2</sup>

Six days after the incident, given persistent complaints of light aversion consistent with photophobia, the soldier was taken to Bagram Air Base for the encouraged ophthalmologic assessment. The exam revealed no ophthalmologic anomalies. Notwithstanding this clinical finding, it was a significant exposure that disabled the driver, causing the crew to break the seal of the vehicle to swap drivers, and exposing the occupants to the threat of small arms fire.

This incident highlights multiple factors involved in a laser ocular exposure, which define the impact on soldier survivability. These factors include the laser source, the visual task, the ambient light conditions, and, beyond the biophysics, the individual concerns over perceived hazard.<sup>3,4</sup> The latter modulates the soldier’s and command’s reactions to the event, influencing “return to duty” determinations, which in turn impact unit readiness.

Perceived hazard phenomenon and laser-induced ocular damage are discussed in detail in other chapters in this volume (see Chapter 7, Psychological and Operational Impacts of Military Lasers, and Chapter 9, Laser-Induced Ocular Effects in the Retinal Hazard Region). This chapter will focus on entoptic laser effects that cause visual disruption but do not cause tissue damage. Many laser incidents involve exposures that temporarily disrupt vision. These incidents typically involve the use of handheld laser pointers, which are often implicated in illuminating aircraft cockpits,<sup>5</sup> moving vehicles, and the faces of individuals such as performers and athletes.<sup>6</sup> Effects on the visual system depend on the retinal illuminance,<sup>7</sup> retinal location affected, extent of retinal area affected, effects of photolysis on retinal neural elements,<sup>8</sup> ambient light-

induced visual function adaptation, and degree of forward scatter on the retina.<sup>9,10</sup> In healthy eyes, some intraocular backscatter does occur, but the effect on vision is nominal, mainly influencing the number of photons that reach the retina.<sup>11</sup>

When assessing the question of laser-induced damage, only the portion of the laser beam directly focused on the retina is considered because this is the area associated with the highest incident energy per unit area. However, along with the beam's directed-energy umbra is an associated penumbra, which is defined by

forward scatter of the beam as it passes through ocular media to the retina. Because this chapter's focus is on vision and visual performance, a model for the effects of bright laser sources on visual function is presented that includes the effect of forward scatter. The model is derived from a Monte Carlo method developed by Jacques and Wang in 1995 for modeling light transport in tissue.<sup>11</sup> The model was adapted by Jonathan M. Ness (chapter author) and is validated against a series of studies that induced retinal light-limiting ocular responses to study the effects of bright laser light on pursuit tracking.<sup>12</sup>

## ENTOPTIC LIGHT-LIMITING RESPONSES

Induced retinal light-limiting ocular responses of the healthy eye involve two physiologic mechanisms: (1) cortically mediated light-limiting responses and (2) a subcortically mediated photic blink reflex. The photic blink reflex is differentiated from the startle blink response, which is a binocular response to unexpected, transient noxious stimuli (eg, loud noise, touching, and visual loom),<sup>13,14</sup> and from the light aversion response, photoallodynia.<sup>15</sup> Photoallodynia is excluded because it is a syndrome that manifests subsequent to intense bright light exposure, which involves trigeminal sensitization.<sup>16</sup> The postexposure tearing in the case of the driver indicates a trigeminal sensitization. Tearing reflex is governed by the fifth (trigeminal) cranial nerve.<sup>17</sup>

### Photic Blink Reflex

There is a continuum of light-limiting responses in the human eye, ranging from pupillary responses to photic blink reflex. Light-limiting responses, save the photic blink reflex, serve to maintain visually guided behavior by mitigating the entoptic effects of bright light on vision. Exposure to extremely bright light sources that subtend a significant retinal area will induce the photic blink reflex, a subcortically mediated reflex that has two myogenic components affecting the orbicularis oculi muscle via the seventh (facial) cranial nerve.<sup>14,17</sup> The first component is a blink onset component that is 30 milliseconds in duration with an average onset latency of 50 milliseconds from stimulus onset. This component is referred to as R50 and is followed by a second burst around 80 milliseconds from stimulus onset, referred to as R80. The R80 impulse persists for about 100 milliseconds, with persistence dependent on light intensity. The behavioral referent for the photic blink reflex described in the literature is a "screwing up of the eyes"<sup>18</sup> caused by the contraction of the orbicularis oculi, which is a sphincter muscle.

The impulse for the photic blink reflex appears to arise when light stimulates melanopsin in intrinsically photoreceptive retinal ganglion cells (ipRGCs). Signals from the ipRGCs serve as primary input for nonvisual photo-regulated physiology such as the pupillary light reflex, blink reflex, irradiance detection, photo-entrainment of circadian rhythms, and, in mice, light suppression of diurnal locomotor activity.<sup>19,20</sup> The photic blink reflex is inhibited by a centrally governed (cortical) tonic levator palpebrae superioris contraction innervated by the third cranial (oculomotor) nerve. The contraction maintains upper eyelid opening and provides voluntary control over eyelid opening and closing. The tension between the subcortical mechanism of the photic blink reflex and the central mechanisms of the light-limiting response determines the continuum of behavioral outcome from nominal pupillary constriction to prolonged eye closure. An intermediary "squinting response" is an orbicularis oculi contraction of the lower lid, with the upper lid remaining open.

Light intensity incident on the retina peaking at 490 nm drives the nonvisual subcortical mechanism, and luminance (perceived brightness) drives the cortical mechanism.<sup>21</sup> A visual photo-regulated inhibitory circuit links the cortical and subcortical mechanisms by way of the ipRGCs. Thus, ipRGCs are influenced by the entire visual spectrum and, in this way, are considered irradiance detectors.<sup>21,22</sup>

In visual photo-regulated physiology, rods and cones depolarize in on- and off-light channels, whereas the nonvisual photo-regulated physiology of ipRGCs responds only to light-on channels. The ipRGCs have an inhibitory circuit from the rod and cone light-on channel. The implication is that the degree of bleaching of the photo elements of the on-circuit determines the inhibition of the ipRGCs. The higher the retinal illuminance and the greater the affected retinal area, the greater the bleaching and the weaker the inhibitory signal, and thus the greater the ipRGC light suppression signal for induction of photic blink reflex.

Bleaching is determined by retinal illuminance measured in  $\log_{10}$  Td·sec (troland-seconds). A troland is a measure of the amount of light energy reaching the retina, normalized to retinal sensitivity for transducing that energy. For a source duration longer than 1 second at a retinal illuminance of  $6.8 \log_{10}$  Td·sec, the fraction of unbleached pigment is 50%, with complete opsin bleaching at  $8.0 \log_{10}$  Td·sec.<sup>23</sup> In a synthesis of research on the photic blink reflex as induced by an incoherent source, Stuck supports the hypothesis that in order to reliably stimulate a photic blink, the source must illuminate a retinal area greater than the rod-free zone at about  $6 \log_{10}$  Td·sec.<sup>24</sup> As the light source was moved in eccentricity from the fovea to the periphery, the latency to blink in response to source onset increased. This increase appeared to correspond to the time the eye responded with a saccade to move the source from the peripheral eccentricity to central fixation. Thus, latency to elicit a photic blink appeared dependent on recruitment of the rod and cone system, since photic blink latency differences across eccentricity correlated with saccade velocity to central fixation.

### Spot Size to Intensity Relationship in Photic Blink Reflex

Few studies can be found that relate laser retinal spot size to intensity in inducing the photic blink response. Regardless, there is considerable debate as to whether the blink reflex should be included as a safety factor in exposure to bright laser light.<sup>25,26</sup> This section is a metaanalysis of refereed journal articles from which retinal spot size, retinal illuminance, and probability of blink may be estimated.

Visible laser light produces high retinal illuminance but relatively small focused spots, which are on the order of 50 to 100  $\mu\text{m}$ . Because of their small spot size, laser sources are unlikely to elicit the photic blink reflex. The studies reviewed here show that the onset of the light source elicits light-limiting behaviors to maintain visual function, which in turn mitigates induction of the photic blink reflex. That mitigation results in about a 15% chance of a blink within 250 milliseconds of light onset, with 5% of those blinks likely spontaneous and, thus, not elicited.

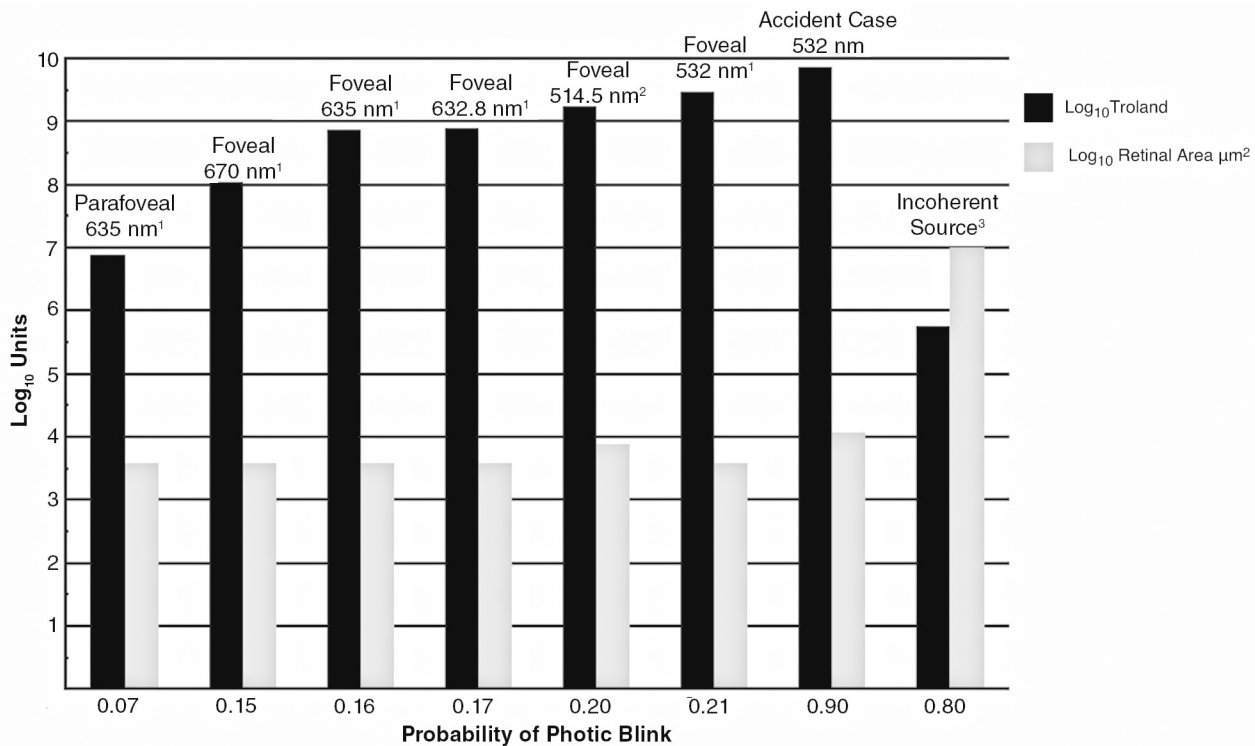


**Figure 6-1.** Probability of photic blink as related to retinal illuminance, retinal spot size, retinal location, and wavelength based on data from an accident case and from three experimentally controlled exposures.<sup>1-3</sup>  
 (1) Reidenbach H-D, Hofmann J, Dollinger K. Active physiological protective reactions should be used as a prudent precaution safety means in the application of low-power laser radiation. In: Magjarevic R, Nagel JH, eds. *World Congress on Medical Physics and Biomedical Engineering*. IFMBE Proceedings. 2006;14:1, 2690–2693. (2) Stumper DA, Lund DJ, Molchany JW, Stuck BE. Binocular and monocular laser glare effects on eye blink and tracking performance. Paper presented at: 25th Annual Lasers on the Modern Battlefield Conference; February 2004; Brooks City-Base, TX. (3) Gerathewohl, S, Strughold H. Motoric responses of the eyes when exposed to light flashes of high intensities and short duration. *Aviat Med*. 1953;24:200–207.

Figure 6-1 shows data from the accident case described at the beginning of this chapter and from three laboratories where researchers have explored the photic blink reflex.<sup>26-28</sup> This figure indicates wavelength dependence; wavelengths closer to peak luminous efficiency (550 nm) are associated with a higher probability of eliciting a photic blink. The apparent anomaly is the parafoveal exposure at 635 nm. However, peak luminous sensitivity in the parafovea is 507 nm, and, thus, a 635 nm stimulus is a less efficient stimulus for parafoveal receptors than for foveal receptors.

Figure 6-1 depicts a retinal illuminance relationship with the probability of a blink increasing with retinal illuminance. There is also an apparent spot-size relationship as indicated in comparing the 514.5 nm and 532 nm spot sizes with that of the accident case. The accident case retinal spot size is 30% and 60% greater than that of the 514.5 nm and 532 nm experimentally controlled exposures, respectively. Note that the retinal illuminance for the incoherent source, estimated at  $5.75 \log_{10}$  Td-sec, is about three orders of magnitude less than the accident case. However, like the accident case, the exposure was delivered as an intense flash, which would reduce opsins to about 45% of the baseline.<sup>8</sup> Moreover, the diameter of the retinal spot produced by the incoherent source encompasses the entire macula ( $\approx 2,800 \mu\text{m}$ ). Those produced by the laser sources are on the order of  $100 \mu\text{m}$  (or about  $\frac{1}{28}$  the diameter of the macula and  $\frac{1}{3}$  the diameter of the fovea).

Although the parameters of spot size and illuminance are identified as likely important to the induction of a photic blink, the relationships are far from clear and require further systematic investigation. From the blink data shown in Figure 6-1 and the breadth of oculomotor light-limiting behaviors in response to bright light reported in the referenced studies, it appears that given the small spot sizes of a focused beam, a quintessentially visual organism engaged in visually guided behavior tends not to blink. Although the focused beam for the accident case was well within the fovea, there were significant postflash sequelae, suggesting that the spot size contributed to the induction of the postflash sequelae. The increase in spot size was likely due to intraocular scatter, which is not accounted for in the NOHD calculation (see Chapter 9, Laser-Induced Ocular Effects in the Retinal Hazard Region, this volume).

Moreover, given the intensity, an appreciable number of pigmented molecules likely received a second quantum hit, disrupting reestablishment of active protein sites on the photoreceptor.<sup>29</sup> Thus, recovery of visual function in the accident case would involve not only recovery of opsin, but also recovery of the active sites that hold the opsin. This effect, called the  $\theta$  effect, is described by Rushton.<sup>8</sup> Recovery in this

case is likely proportional to the number of photons delivered by the source, rather than to the amount of visual pigment bleached.<sup>29</sup>

### **Pupillary Responses, Partial and Monocular Lid Closure, and Eye Movement**

Short of the induction of the photic blink response, the visual system exhibits a breadth of retinal light-limiting behaviors. These behaviors include pupillary reflex, eye movement, closing one eye, squinting, and blinking. The pupillary reflex is governed by the ipRGCs specifically associated with the R80-myogenic impulse.<sup>30</sup> The pupillary reflex is also centrally governed, influenced by true luminance scene changes as well as by changing visual illusions of brightness.<sup>31</sup>

The pupillary reflex and blink reflex show a summation of a binocular signal due to the crossing visual ascending pathways of the nasal retinal ganglion cells.<sup>14,32</sup> An equivalent monocular sensation of brightness reported under binocular viewing requires an order of magnitude increase in light intensity, provided the stimulus is on for more than 1 second.<sup>32</sup> Under binocular exposure conditions, a light-limiting behavioral response is to close one eye.

The eye is constantly moving, with eye movements contributing to the smear of energy on the retina. Under deliberate fixation of a diffraction-limited spot at optical infinity, eye movements produce about a  $50 \mu\text{m}$  diameter spot on the retina. Viewing a focal target for longer than 1 second, the spot increases to  $150 \mu\text{m}$  with the inclusion of head movement.<sup>33</sup> Accounting for head and eye movement, peak radiant power is reduced by one-thirtieth of the expected power for the no-movement case.<sup>33</sup>

### **Effects on the Resolving Power of the Eye**

Fixation on target distinctive features is contrast dependent, with the eye focusing on areas of high contrast and features that are spatially resolvable by the eye. With a masking bright light source, the fixation tends to move off of the source to a target area resolvable by the eye (see Chapter 5, Laser Glare Effects on Visual Performance, this volume). By virtue of redirecting fixational gaze, the relative luminous efficiency of the source decreases as a function of its distance from the pupil center.<sup>34</sup> Viewing a source at the margin of a 3 mm pupil reduces luminous efficiency by 20%, making the source appear less bright. For laser exposures longer than 1 second, the viewer can adjust fixation to eccentric viewing of the target, which preserves visually guided behavior by diminishing the perception of source brightness. In this way, the masking bright light source contributes to reduc-

ing sensitivity of the eye not only through bleaching opsins, but also through inducing the movement of target fixation from the masked target to some other associated feature of the target resolvable by the eye.

In the visual photo-regulated physiology, ambient light levels and degree of photolysis determine the recovery of visual function and persistence of after-images. The affected retinal area determines the suppression of visual function. Figure 6-2 shows contrast sensitivity (1/% contrast) as a function of target size for four conditions of stabilized opacity in the visual field. The opacity simulates effects of afterimages and of masking bright light sources on the resolving power of the eye. The “No Scotoma” condition shows visual function within normal limits under typical photopic viewing conditions. The “5° Foveal” condition simulates the effect of an afterimage centered on the fovea, occluding the central 5° of vision. The “2° Parafoveal” condition simulates the effect of an afterimage outside the macula, occluding 2° of peripheral vision. The “5° Relative” condition simulates the effect of a masking bright light source centered on the fovea, reducing contrast by 5% in the central 5° of vision.

Figure 6-2 also shows that relative to the “No Scotoma” condition, the central occlusions had a greater effect on high- to mid-spatial frequencies, whereas the

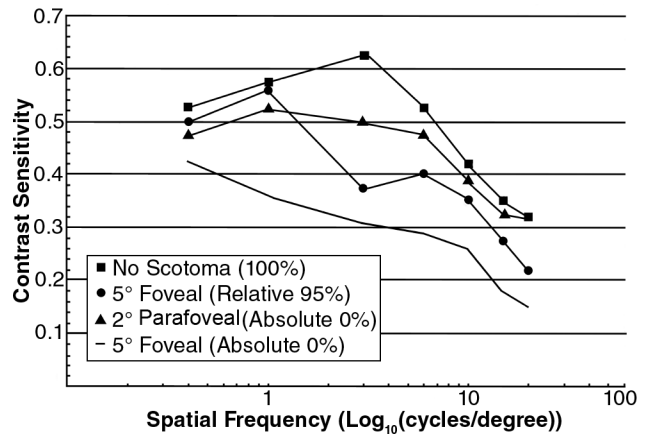


Figure 6-2. Contrast sensitivity as a function of target size for four conditions of stabilized opacity in the visual field.

peripheral occlusion had a greater effect on low- to mid-spatial frequencies. Note that regardless of retinal position, all occlusions induced a significant suppression of sensitivity in the mid-spatial frequencies. This tendency may implicate that mid-spatial frequency sensitivity is a result of a neural integration of peripheral and central retinal signals along the visual pathway.<sup>35,36</sup>

### MODELING INTRAOCULAR SCATTER

When viewed intrabeam, a laser source appears as a small bright spot surrounded by a halo of diffuse light (Figure 6-3). This section introduces a model of intraocular scatter to define the extent of the penumbra of retinal illuminance surrounding the umbra, or small bright spot. This intraocular scatter is separate from scene glare. Scene glare, as depicted in Figure 6-3, is caused by reflections from a glare source incident with the scene, which disrupts scene contrast (see Chapter 5, Laser Glare Effects on Visual Performance, this volume).

Laser-induced intraocular scatter is wavelength dependent for viewing angles less than 4°. <sup>10</sup> A viewing angle of 4° equates to a retinal extent of about 70 mrad, or about twice the extent of the rod-free zone (Figure 6-4). The focused beam of the laser described in the accident case was about 0.4°, which equates to a retinal extent of about 7 mrad. <sup>10</sup> Although the effects of scattering are minimized in the optics of the cornea and lens, and through waveguide at the retina, the optics of the eye leave longitudinal chromatic aberration uncorrected. <sup>37</sup> Thus, the wavelength results in differential effects on image quality. For wavelengths greater than 600 nm, there is increasing diffusion, which increases the spread of the point-spread function, defocusing the

image. <sup>10</sup> For wavelengths less than 600 nm, there is an increasing effect of scatter. <sup>10</sup> Ginis and colleagues report that, at a viewing angle within 0.5°, the effect of straylight can be five times higher in the red seg-



Figure 6-3. Laser glare veiling a target acquired through targeting optics. The veiling glare is from a laser source mounted on an armored vehicle directed at the viewing optics of a tube-launched, optically tracked, wire-guided missile system targeting the armored vehicle.

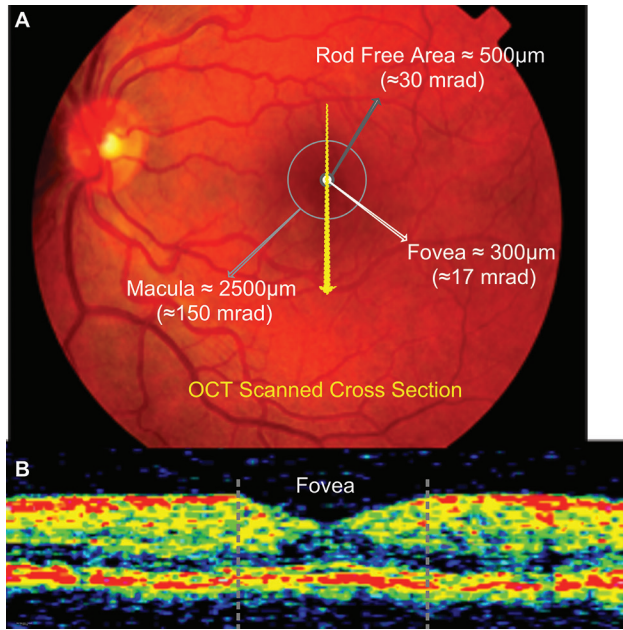


**Figure 6-4.** (a) The diameter in µm of the fovea, rod-free area, and macula, and their respective angular subtenses in mrad. (b) Optical coherence tomography (OCT) image showing a full retinal thickness cross-section of scanned retina.

ment of the visual spectrum (> 600 nm) than in the green (500–575 nm), implicating the role of straylight in chromatic induction.<sup>10</sup> For example, there is a tendency to see a red hue in the glare from white light sources.

**TABLE 6-1**  
**DISTANCE AND TISSUE LAYER THICKNESS**  
**USED TO PREDICT INTRAOCULAR SCATTER**

Boundary layer	Thickness of tissue (mm)	Distance from front of cornea (mm)
Cornea	0.5	0.5
Aqueous/anterior chamber	3.1	3.6
Lens capsule 1	0.01	3.61
Crystalline lens	3.58	7.19
Lens capsule 2	0.01	7.2
Vitreous humor	17.2	24.4
Macula lutea/ Henle fibers	0.03	24.43
Retina	0.47	24.9
RPE	0.02	24.92

RPE: retinal pigment epithelium

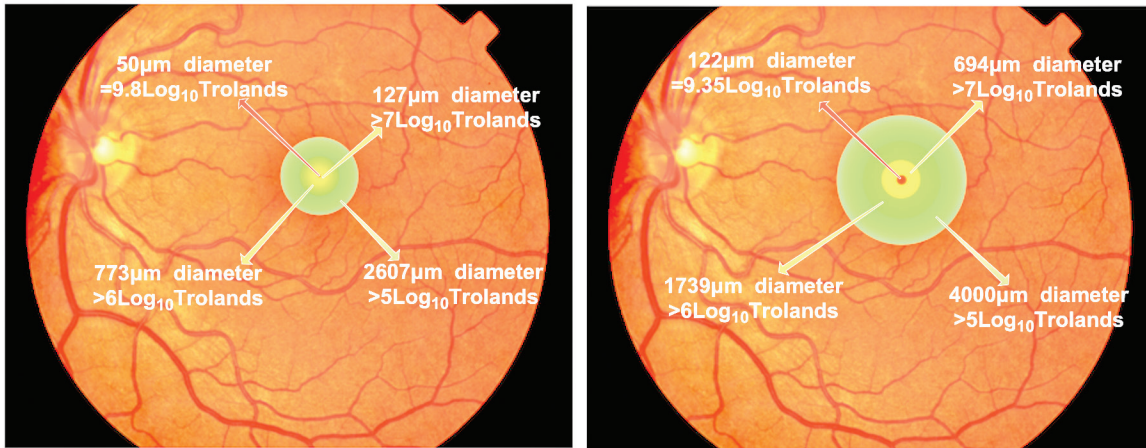
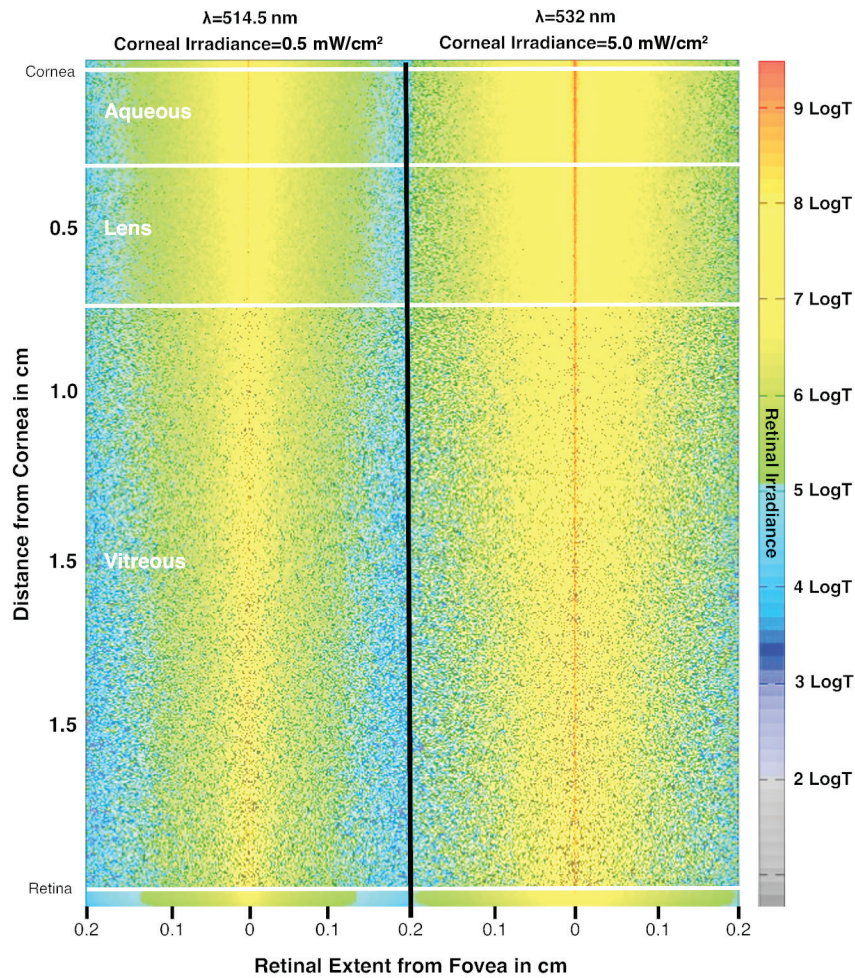
To estimate the effective spot size of a laser source on the retina, which includes scattering and diffuse reflectance, the contribution of each boundary layer of the eye to the path of a photon was computed from cornea to retinal pigmented epithelium. Table 6-1 shows each of the boundary layers used in the model, with the associated tissue thicknesses and distance from the corneal surface. The model incorporates each layer’s refractive index, coefficient of absorption, scatter coefficient, and anisotropy. Absorption, scatter, and anisotropy are wavelength dependent. As a photon interacts with each layer, the algorithm determines if there is a drop in the energy weight of the photon and then determines its deflection angle and azimuth of travel.

Figure 6-4 shows the extent of retinal structures as a reference for Figure 6-5. Figure 6-5 depicts the illuminance, through the layers of the eye, as a heat map of the laser power incident at the cornea for the reported accident case and for the 514.5 nm controlled experimental exposure reported by Stamper and colleagues.<sup>38</sup>

Figure 6-5 also illustrates the effect of scatter on retinal spot size (it does not show the extension of the retinal spot due to retinal smearing produced by head and eye movements). The figure shows a focusing of the beam in the lens and a broader area of high illuminance in the anterior chamber, producing considerable veiling glare. Within the vitreous, there is relatively broader scatter due to the lower anisotropy associated with the vitreous. At the boundary of the vitreous and the retina, there is a significant energy absorption that defines the umbra of absorption due to the focused beam (red spot) and the penumbra of absorption due to scatter (yellow to green annuli).

The illuminance of the umbra for the 514.5 nm beam<sup>38</sup> (see Figure 6-5, left panel) is  $9.3 \log_{10}$  Td, and that of the 532 nm beam associated with the accident case (see Figure 6-5, right panel) is  $9.87 \log_{10}$  Td. The corneal irradiance of the 532 nm beam is an order of magnitude greater than that of the 514.5 nm beam. The 514.5 nm focused spot is 50 µm for 3.0 seconds, and that of the 532 nm spot is 122 µm for 0.1 seconds. These differences contribute to the extent of the respective associated penumbras due to intraocular scatter.

In addition, Figure 6-5 shows that the extent of the penumbra out to  $6 \log_{10}$  Td for the 514.5 nm beam is 2,600 µm. This equates to a 5 mm<sup>2</sup> retinal area. The extent of the penumbra out to  $6 \log_{10}$  Td for the 532 nm beam is 4,000 µm. This equates to a 12 mm<sup>2</sup> retinal area, which is twice the area produced by the 514.5 nm source and equivalent to that of the incoherent source (see Figure 6-1). Given the increased retinal area affected by the 532 nm source due to intraocular



**Figure 6-5.** Light scatter around the focused beam (red) traveling from the cornea to the retina for a 514.5 nm, 0.5 mW/cm<sup>2</sup> controlled exposure reported by Stamper et al<sup>1</sup> and for a 532 nm, 5 mW/cm<sup>2</sup> accident case exposure. Focused beam spot sizes for the 514.5 nm beam and the 532 nm beam are 50 μm and 122 μm, respectively. The > 5 log<sub>10</sub> Td illuminance penumbra around the 514.5 nm focused beam spot and 532 nm focused beam spot are 2,607 μm and 4,000 μm, respectively.

(1) Stamper D, Lund D, Molchany J, Stuck B. Laser-induced afterimages in humans. *Percept Motor Skills*. 2000;91:15–33.

scatter, the probability of blink is estimated to be greater than the probability associated with the incoherent source (see Figure 6-1).

In Figure 6-5, the penumbra was estimated out to over  $6 \log_{10}$  Td illuminance, based on Rushton's finding<sup>23</sup> that 50% of the opsins are depleted, from

an adaptive state baseline, at a retinal illuminance of  $6.8 \log_{10}$  Td·sec. In general, the opsin bleaching for a given retinal illuminance follows a Weber-Fechner constant, from which contrast sensitivity and the duration and intensity of afterimages can be predicted.<sup>39,40</sup>

## SCATTER MODEL VALIDATION

In 1979, when a team of vision scientists at Letterman Army Institute of Research was confronted with the question of how intense, sub-injury threshold laser light might affect soldier performance, they chose to study the effects of laser-induced visual disruption on pursuit-tracking behavior. Tracking behavior is visually guided and also involves the integration of other sensory inputs (eg, proprioceptive and vestibular) to maintain orientation. The scientists recognized that laser disruption to visually guided behavior would be expected to cause performance deficits, but that individuals may be able to compensate and adapt to the visual disruption. Disruption of the visual signal was predicted to alter sensory integration and to induce behavior (eg, blinking, pupil constriction, and eccentric viewing) that would limit retinal illuminance. To test their predictions, the research team developed the Blaser system.<sup>41-43</sup>

### Blaser Visual Pursuit System

In 1985, Peter O'Mara, David Stamper, David Lund, Richard Levine, Bruce Stuck, and Edwin Beatrice conducted the first purposeful, nonclinical study of human laser exposure.<sup>44</sup> Volunteers engaged in a pursuit-tracking task were exposed to low levels of visible laser light (below the MPE level). The results provided timely answers concerning the relationship between laser source and target parameters, and their effects on visual performance. The investigators found that when equal amounts of laser energy from 514.5 nm argon-ion (Ar) and 632.8 nm helium-neon (HeNe) lasers were presented to volunteers as they performed a pursuit-tracking task, the 514.5 nm laser light (near the peak of the photopic sensitivity curve) was relatively more disruptive. Continuous wave (CW) laser exposures were also compared to repetitively pulsed (RP) lasers exposures. For RP durations of up to 30 Hz, the CW mode of presentation was the more disruptive.

Figure 6-6 is a schematic showing the current version of the Blaser tracking simulator, which includes an option for binocular or monocular viewing.<sup>45</sup> The Blaser scene subtends a visual angle of  $12.7^\circ$  and can be adapted to accommodate ambient lighting and figure/ground contrast for the tracking task. The tracked

target is a  $1/35$  scale model tank that subtended  $2^\circ$  ( $35$  mrad) of visual angle. The target moved alternately left-to-right and right-to-left in a fixed arc, at  $0.28^\circ$  per second angular velocity at a simulated distance of 2 km. To maintain velocity and simulated distance, the model tank was moved along an HO-gauge model train track. A square aiming patch housed the detector that measured tracking accuracy. The patch subtended 2 mrad with a black center dot about 1 mrad in visual angle. The desert camouflaged model tank was set against a desert scene background. The beam from the Ar (514.5 nm) laser source was brought into the eyepiece through a fiber optic cable. Exposures were limited to approximately 40% of the MPE, with a retinal illuminance of  $9.1 \log_{10}$  Td over a  $50 \mu\text{m}$  retinal diameter focal spot.<sup>46</sup>

### Photoreceptor Bleaching and Performance

Light energy incident on the retina is transduced as chemical energy through absorption of photons by opsins in the photoreceptors. The absorption leads to bleaching of the opsin, which in turn generates an electrical potential. Through a complex of enigmatic



**Figure 6-6.** A Blaser tracking simulator with binocular viewing capability used at the Walter Reed Army Institute of Research in the 1990s.<sup>1</sup>

(1) Stamper D, Lund D, Molchany J, Dembrowsky, Boneta O, Stuck B. *Validation of the Blaser II Laboratory Tracking System*. Silver Spring, MD: Walter Reed Army Institute of Research; 1997. Technology Report 97-001.

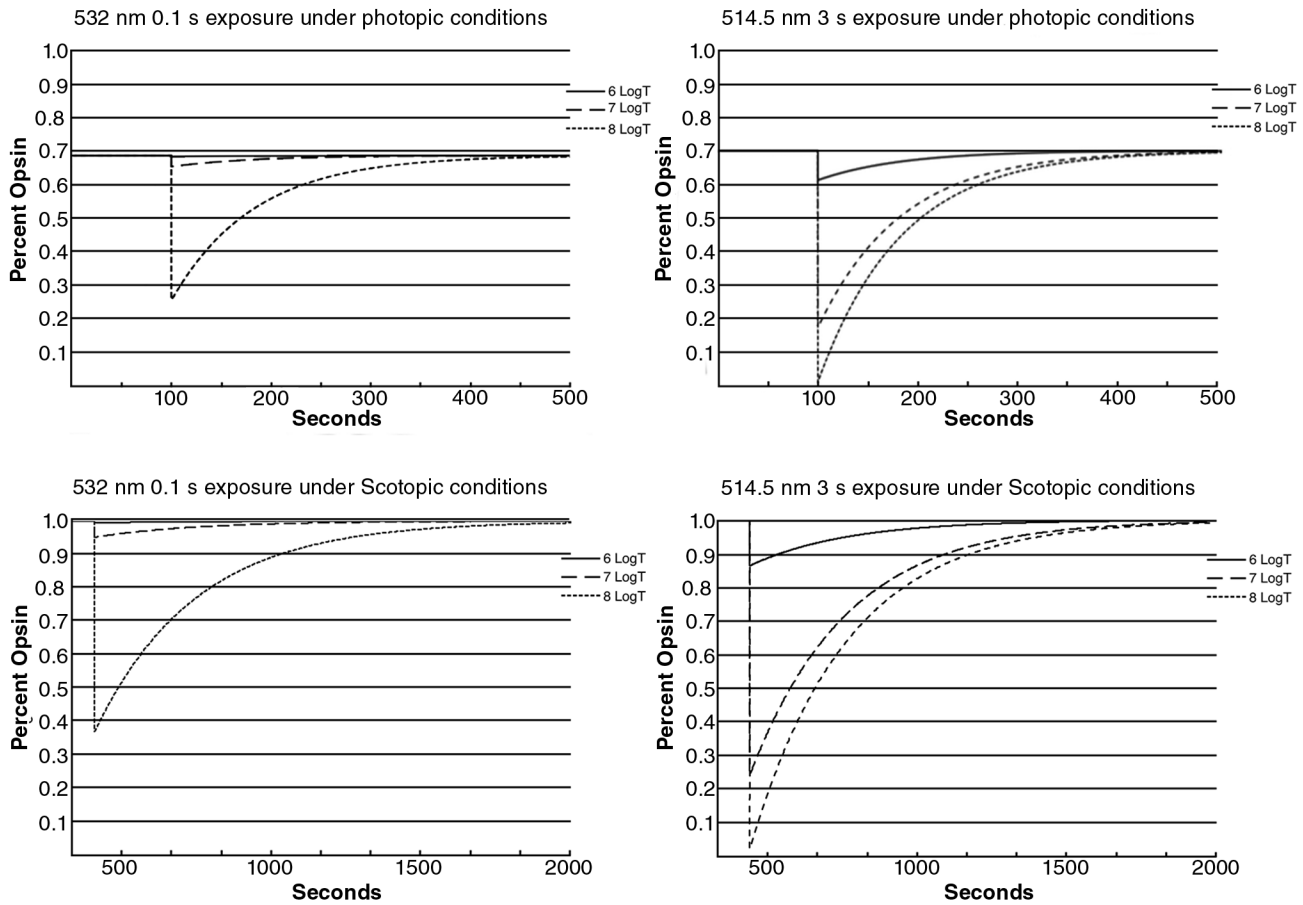


**Figure 6-7.** Photopic (cone) and scotopic (rod) bleaching and recovery Rushton curves for a 532 nm accident case exposure and a 514.5 nm Blaser exposure. Penumbra annuli around the focused beam umbra associated with 6, 7, and 8  $\log_{10}$  Td (see Figure 6-5) show degree of bleaching and time to return to baseline. Note that the 532 nm source duration is 0.1 seconds for both accident case curves, and the 514.5 nm source duration is 3 seconds for both Blaser curves.

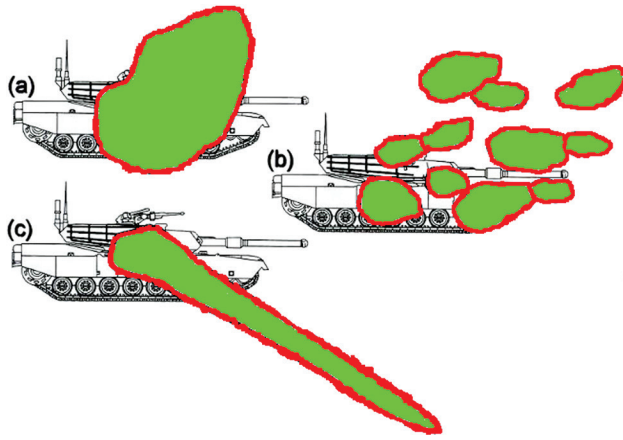
neural entanglements well beyond the scope of this chapter, the transmitted electrical pulse durations, rates, and intensities manifest as conscious visual perception. For light sources that do not induce a flash photolysis effect,<sup>8</sup> the extent of opsin bleach depends upon retinal illuminance as well as retinal exposure duration.

Figure 6-7 shows the cone bleaching and recovery curves for the 532 nm accident case exposure (left panels) and for the 514.5 nm Blaser exposure (right panels). The upper charts are the photopic recovery curves and the lower charts are the scotopic curves. Each chart shows percent opsin remaining or bleached as a function of time. The curves show laser onset at 100 seconds and plot bleaching and recovery for the retinal areas associated with 6, 7, and 8  $\log_{10}$  Td retinal illuminance. The difference in bleaching efficiency is related to the amount of time the retinal area was illuminated. The 532 nm source illuminated the retina for 0.1 seconds,

and the 514.5 nm source illuminated the retina for 3 seconds. The graph for the 514.5 nm exposure indicates that the retinal area inclusive of 7  $\log_{10}$  Td bleaches opsins to within 50% of baseline. The associated retinal diameter (as described in Figure 6-5) is 127  $\mu\text{m}$ , which corresponds to a visual angular subtense of 7.25 mrad. The Blaser target subtended 35 mrad, which is about five times that of the visual angular subtense associated with 50% opsin bleaching for the 514.5 nm source.

**Light-Limiting Strategies Revealed in Patterns of Afterimages**

Figure 6-8 depicts the pattern of afterimages as recorded on an Amsler grid from volunteers who were exposed to the 514.5 nm source for 3 seconds during a pursuit-tracking task in the Blaser simulator. The figure indicates three strategies used to maintain tracking performance. Figure 6-8a depicts a strategy



**Figure 6-8.** Illustrations of the differing patterns of afterimages reported (a) when an observer stared at a laser without blinking, (b) when the observer repeatedly blinked when the laser was on, and (c) when the observer made a rapid eye movement away from and back to the target aiming point.

to maintain fixation on the aiming point. This strategy would yield significant retinal smearing due to head and eye movement over the 3-second exposure.<sup>33,47</sup> The expected effect of smearing is to increase the 127  $\mu\text{m}$  spot by 150  $\mu\text{m}$ , producing a total spot size diameter of 277  $\mu\text{m}$ . Because bleaching is dependent on exposure time, the movement would interrupt dwell time on any given retinal spot until revisited. Average dwell time for a given fixation over the 3-second exposure is 0.15 seconds.<sup>33</sup> Thus, the opsin bleaching and recovery would be consistent with the function for the 532 nm photopic function (0.1 s exposure) and would follow the same afterimage persistence timeline as described for the blinking strategy (Figure 6-8b).

Figure 6-8b depicts the afterimages from a volunteer who reported “rapidly blinking” during the laser exposure.<sup>38</sup> Latency for a blink response, at its limit, is 250 milliseconds.<sup>48</sup> Over 3 seconds, at a rate of four per second, there should be about 12 spots given a constant blink rate. Figure 6-8b shows 11 afterimage spots with an angular subtense between 7 and 10 mrad. The spot left of the bore evacuator at the fore of the turret is over the aiming point, which is the spot of best fixation on the aiming point. This spot measures 7 mrad as predicted in Figure 6-5 (left panel, 7  $\log_{10}$  Td spot). A nominal effect of smearing of the spots is expected due to head and eye movement. The shorter effective exposure times would likely result in bleaching and recovery function closer to 8  $\log_{10}$  Td curve for the 532 nm photopic condition (see Figure 6-7). The curve predicts that the time to recover 50% of the bleached

opsins is 70 seconds, which is about the time the afterimage should persist under photopic conditions.<sup>40</sup> Time to fully recover to baseline is 300 seconds. Note that in the scotopic curves for all three cases, if the volunteers close their eyes (effectively producing a scotopic background condition), the reintegration of the afterimage with eye closure is predicted to occur up to 400 seconds postexposure.<sup>40,49</sup>

Figure 6-8c depicts a saccade to inferior-temporal space relative to and away from the source. Thus, the source was placed in the superior-nasal visual field. As described earlier in this chapter, viewing the source in this manner reduces luminous efficiency by 20%. The exposure was a monocular right-eye exposure, which in retinal space would mean that the laser source was placed on the inferior-temporal retina. Curcio and Allen reported that “densities in nasal retina exceed those at corresponding eccentricities in temporal retina by more than 300%; superior exceeds inferior by 60%.”<sup>50(p5)</sup> Thus, as a result of the eye movement, the laser source was placed in a relatively low receptor area. The saccade is estimated to be about 40 mrad, which is beyond the rod-free area around the fovea (see Figure 6-4), resulting in the illumination of a 700  $\mu\text{m}$  path of photoreceptors from the fovea along the inferior-temporal path shown in Figure 6-8. Given the distance, the saccade would include about a 200-millisecond onset and take about 70 milliseconds to travel the distance and return.<sup>51</sup> The width of the streak is consistent with the spot size estimate from the scatter model. However, since saccadic eye movements were not reported in the Blaser study, it is difficult to assess retinal effects beyond inferences from spot sizes as reported in Figure 6-8.

### Pupillary Response and Performance

Associated with the onset of the laser is a concomitant, compensatory change in vision that diminishes retinal illuminance and glare. Glare effects end with glare source termination (see Chapter 5, Laser Glare Effects on Visual Performance, this volume). However, the effects of retinal illuminance persist, with retinal function recovering per the opsin recovery depicted in Figure 6-7. The effect of the laser is dependent on the adaptive state of the eye and characteristics of the laser source.<sup>52</sup> As shown in Table 6-2 and Figure 6-8, the calculated retinal illuminance is greatest at the onset of the source and diminishes with light-limiting pupil adaptations and oculomotor behavior.

Table 6-2 shows pupillary changes for 0.1- and 3-second exposures for photopic and scotopic ambient conditions. These data confirm the effect of binocular summation in the pupil response as considered in the earlier discussion of light-limiting behavior. In

TABLE 6-2

PUPIL DYNAMICS IN RESPONSE TO LASER OCULAR EXPOSURE DURATION, AMBIENT LIGHT CONDITIONS, AND VIEWING CONDITIONS

	Bright				Dim			
	Monocular		Binocular		Monocular		Binocular	
Duration (s)	0.1	3.0	0.1	3.0	0.1	3.0	0.1	3.0
Baseline (mm)	6.3	6.5	5.2	5.6	7.3	7.3	7.0	7.0
Minimum (mm)	3.9	2.9	3.5	2.5	4.5	2.9	3.5	2.9
Recovery (mm)	5.7	5.3	4.6	4.2	6.2	5.5	4.9	4.7

response to source onset and at recovery, the pupil diameters at baseline are smaller for the binocular versus the monocular exposures.

Pupil constrictions in response to source onset limits retinal illuminance. For example, the dim-light monocular-viewing condition for the 0.1-second exposure results in pupil constriction from the baseline diameter of 7.3 mm to 4.5 mm. In turn, this change limits light onto the retina and changes retinal illuminance from  $9.9 \log_{10} \text{Td}$  to  $9.5 \log_{10} \text{Td}$ . For the 3-second exposure, the pupil constricted to 2.9 mm, resulting in a reduction of retinal illuminance to  $9.1 \log_{10} \text{Td}$ .

Figure 6-9 shows the mean performance of volunteers engaged in the Blaser pursuit-tracking task. Exposure conditions and retinal spot sizes for the 0.1- and 3-second exposure durations are as previously described in this chapter. There were robust effects for exposure time and ambient light conditions. Time off target was about twice that for the dim-light conditions compared to that of the bright-light conditions. Comparing pulse durations within viewing (binocular or monocular) and ambient light (bright or dim) conditions, the 3-second exposure produced about a 4-fold increase in time-off-target scores compared to the 0.1-second scores. Time off target was shorter for binocular viewing compared to monocular viewing, with the differences particularly pronounced under dim-light conditions.

From the data reported in Table 6-2, the effect of summation in the binocular case resulted in smaller pupil sizes, effectively limiting light to the retina. As the performance data suggest, the smaller pupil size is associated with improved performance for the binocular condition compared to that of the monocular condition. The reported data are averaged. The data do not indicate that a light-limiting strategy of closing one eye occurred in the binocular case. The pupil constriction data in Table 6-2 show the expected difference between monocular and binocular pupil constriction, predicted by nasal pathway summation.

**Assessment of Performance and the Entoptic Scatter Model**

Assessing the performance data based on opsin recovery functions (see Figure 6-7), the data show that recovery of pursuit tracking is not well explained by opsin recovery. Time-off-target measures began with the onset of the source and continued until the target was reengaged. Thus, to assess opsin recovery, the duration of the laser exposure was subtracted from the total time off target. For bright-light conditions, the effects of opsin recovery are nominal, given tracking was lost for less than a second. In the bright-light conditions, opsins were bleached to about 45% of baseline, and the bleaching seemed to have little postflash effect on performance. For the dim-light condition for the monocular 3-second exposure, the estimated 4 seconds time off target from source offset ( $\approx 7 \text{ s}$  total time off target; 3-s exposure) yields a 6% opsin recovery to

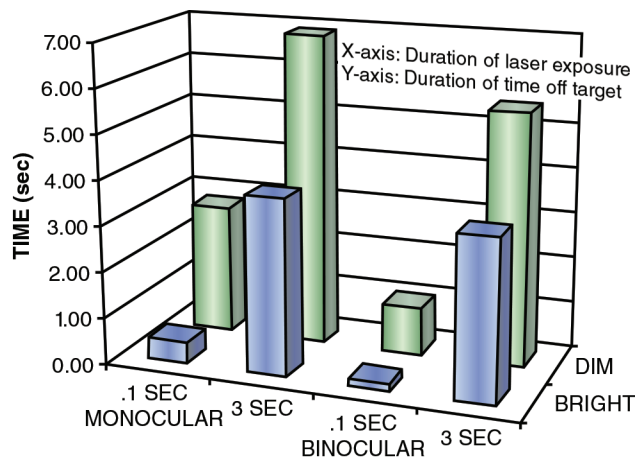
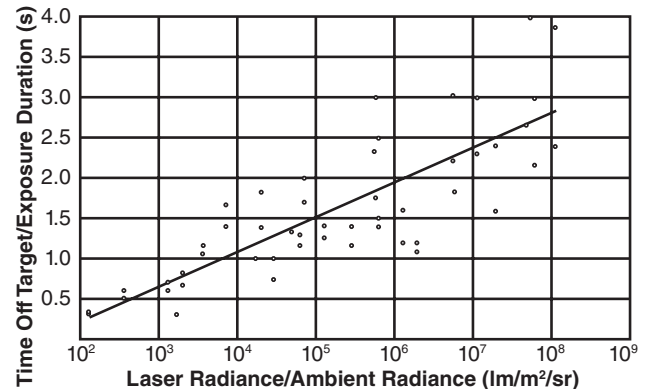


Figure 6-9. Mean performance of volunteers engaged in a Blaser pursuit-tracking task. Average total time off target as a function of viewing condition, laser exposure duration, and ambient lighting conditions.

baseline. Under the dim-light condition, opsins were bleached to about 65% of baseline. Note from the previous eye-movement discussion that the opsin recovery curves are based on a 0.1-second exposure (see Figure 6-7). Similar to the bright-light condition, data for the dim-light condition suggest that opsin recovery was nominally related to the return of pursuit-tracking performance.

The time-off-target data seem to be most parsimoniously explained by two factors: (1) a glare event and (2) the induction of a retinal relative scotoma (after-image). The disruption due to the glare event would last as long as the laser was on. The induction of a relative scotoma depends upon retinal illuminance as described in Figures 6-5, 6-7, and 6-8. In this case, the source produced a central relative scotoma on the order of 127  $\mu\text{m}$  on the retina, corresponding to 7.25 mrad or about 0.4° of visual angle. The scotoma likely affected the ability to resolve mid- to high-spatial frequency targets as described in the curve showing the suppression of the resolving power of the eye for the 5° central relative scotoma (see Figure 6-2). The Blaser target subtended 2° of visual angle, which equates to 0.5 cycles per degree or a low spatial-frequency target. The low spatial-visual channel is mainly governed by parafoveal pathways associated with the magnocellular visual pathways.<sup>53</sup> Although the aiming point is a foveal-resolved target, the aiming point, as referenced by the extent of the tank and its position in the reticle, is resolvable in the parafovea. Together with the smooth track of the target, the recovery of the sensory integration of the visually guided behavior likely accounts for the relatively short latency from laser source offset to recovery of tracking performance. In this way, the bleached patch of opsins and associated afterimage predict overall resolving power of the eye and, thus, the effect on performance.

Taken together and when normalized across exposure times and ambient light conditions, these data show a constant ratio as predicted in a Weber-Fechner



**Figure 6-10.** Graph of data from the Blaser pursuit-tracking task. Time off target is normalized to exposure duration as a function of  $\log_{10}$  laser radiance normalized to ambient radiance. The regression line suggests an underlying constant ratio that follows Weber's constant.

relation (Figure 6-10). The data support the fact that sensation is dependent upon changes in source radiance relative to ambient radiance. The sensation is the underpinning for the perception and behavioral changes. The regression shows a constant in the relationship between effect on visual performance and ratio of laser radiance to ambient radiance. This constant ratio is about 0.45. The caveat is that the correlation coefficient of the curve that fits these data is  $R^2 = 0.35$ . This is likely due in part to the varied light-limiting behaviors used to maintain tracking, which would affect the outcome of pursuit-tracking performance. Also, Weber's law is applied liberally in that the task is intersensory. Visually guided behavior is guided by vision and dependent on visual function, but not uniquely predicted by it. Head and eye movements are coordinated through the inner ear, and motion of the track is aided through proprioception. Despite these caveats, there is a significant underlying visual-sensory mechanism that governs the data, evincing Weber's law.

## CONCLUSION

The overarching finding is that a quintessentially visual organism, when engaged in visually guided behavior, will tend not to blink in response to bright light. To induce a photic blink, a significant area of the macular region has to be illuminated to greater than or equal to  $6.8 \log_{10}$  Td-sec. Based on the data presented in this chapter, it is estimated that this area must at least broach the rod-free zone of central vision (see Figure 6-4; > 500  $\mu\text{m}$  diameter). The focused beam of a laser is typically on the order of

100  $\mu\text{m}$ . Associated with the umbra of the focused beam is its penumbra. The size of the penumbra determines the opsin bleaching of the retina, which in turn depends on wavelength, power incident at the cornea, and ambient lighting conditions. Compared to the experimentally controlled exposures depicted in Figure 6-1, the retinal illuminance of the focused beam associated with the accident case exposure was equivalent to experimentally controlled exposures as reported by Stamper and by Reidenbach.<sup>12,26</sup>

The difference between the accident case and the experimentally controlled exposures is the retinal area affected as predicted by forward scatter. The spot sizes resulting from the addition of the penumbra for the controlled experiments were well within the limit of the rod-free zone, even when accounting for retinal smearing due to head and eye movements. Factoring in the penumbra for the accident case yields a spot size larger than the rod-free zone. For retinal illuminance greater than  $7 \log_{10} \text{Td}\cdot\text{sec}$  ( $6.8 \log_{10} \text{Td}\cdot\text{sec}$  for 50% opsin bleach), the diameter of the illuminated spot for the accident case was 694  $\mu\text{m}$ . The sequelae associated with this exposure were consistent with symptoms of photoallodynia. Exposure in the accident case was dangerously close to the exposure dose associated with a 50% chance of producing a minimally visible retinal lesion ( $\text{ED}_{50}$ ), whereas the experimentally controlled exposures were 40% less than the MPE. The experimental data show a significant repertoire of adaptations to limit light on the retina so as to maintain visually guided behavior. This point is best made by Reidenbach, who advocates a proactive approach to incorporating these behavioral adaptations into the safety standards.<sup>26</sup>

There is the potential that the accident case exposure resulted in what Rushton described as a  $\theta$  effect.<sup>8</sup> From the calculations described by Rushton,<sup>8</sup> the accident case would have received successive quantal hits with average time between successive hits per molecule, about 10 milliseconds over the 100-millisecond exposure. The exposure would have bleached opsins to within 45% of baseline and deformed active-site proteins. The latter effect is unique to the flash photolysis process. The outcome would be a significant increase in latency to recovery of visual function because, along with opsin recovery, active sites must recover conformity to accept the opsin. The biochemical changes have a cascading effect on processes such as lateral inhibition<sup>54</sup> and diffusion of the chemicals that underlie formation of afterimages.<sup>55</sup> Flash photolysis effects, along with those of spot size, may explain the induction of symptoms of photoallodynia experienced by the convoy driver.

The major contribution of this chapter to the assessment of laser tissue interaction is the forward scatter model, which was based on the model developed by Jacques and Wang.<sup>11</sup> The model allows for quantifica-

tion of forward scatter on the retina, which is critical for the assessment of performance-related metrics in laser ocular exposure. The model showed that the ocular system is very efficient in directing photons to the retina and, although scatter does occur, it is centrally directed. For many of the posterior tissue boundaries, the model used bovine coefficients of anisotropy, absorption, and scatter. Thus, this model can certainly be improved upon. The model includes a Henle fiber layer to account for absorption in the blue spectrum. However, wavelengths in that range were not run; the study's objective was to explain the accident case sequelae in contrast to the outcomes of experiments that studied light-limiting behaviors in the context of visually guided behavior. Without the scientists' work in the Blaser program, validation of the forward scatter model would not have been possible; this fact points to the relevance of their work today.

Lasers are currently used and will continue to be used as less-than-lethal means in the de-escalation of violence, particularly in postconflict operations<sup>56</sup> as was described in the accident case from Kabul, Afghanistan. However, the use of lasers as visual disruptors requires a reassessment of beam divergence and power to effectively induce the desired visually disruptive effect. The glare effects are disruptive and last as long as the laser is on. The effects of the induced relative scotoma depend on retinal illuminance and spot size, which in turn depend on viewing conditions, laser output power, and beam divergence. The desired effects are determined by rules of engagement and relevant tactical distances. These effects could range from psychological (eg, "There is a laser spot on me!"; "I am being targeted!") to the symptoms described in the accident case that caused the crew to breach the seal of their vehicle. The available science now allows researchers to reliably model these effects for the appropriate implementation of lasers as less-than-lethal resources in postconflict operations. In these types of operations, the goal is to consolidate the win of the kinetic effort by promoting stability, but the ability to promote stability depends on the ability to limit lethal force where possible. As visual disruptors, lasers provide soldiers another resource to limit lethal force and thus promote stability in postconflict operations.

## REFERENCES

1. Army Public Health Center. *Laser Hazard Evaluation of the B.E. Meyers & Co. Inc., Green Laser Interdiction System Production Model*. Aberdeen Proving Ground, MD; 2011. Nonionizing Radiation Protection Study No. 25-MC-0F2B-11.
2. American National Standards Institute. *American National Standard for Safe Use of Lasers: ANSI Z136.1-2014*. Orlando, FL: Laser Institute of America; 2014.

3. Rockwell JR, Ertle WJ, Moss CE. Safety recommendations for laser pointers. *J Laser Appl.* 1998;10(4):174–180.
4. Ness J. Communicating the risk of weapons of mass casualty. *Combating Terrorism Center Biodefense Rep.* 2006;1(1):10–12. [https://www.files.ethz.ch/isn/26330/ctc\\_biodefense\\_rep\\_june\\_06.pdf](https://www.files.ethz.ch/isn/26330/ctc_biodefense_rep_june_06.pdf). Accessed October 16, 2017.
5. Laser Accident Database. Rockwell Laser Industries website. <https://www.rli.com/resources/accident.aspx>. Accessed October 16, 2017.
6. Non-aviation incidents. Laser Pointer Safety website. [http://www.laserpointersafety.com/news/news/nonaviation- incidents\\_files/tag-car.php](http://www.laserpointersafety.com/news/news/nonaviation- incidents_files/tag-car.php). Accessed October 16, 2017.
7. Kaiser PK. *CIE 1988 2° Spectral Luminous Efficiency Function for Photopic Vision*. Vienna, Austria: International Commission on Illumination; 1988. CIE Publication No. 086-1990.
8. Rushton W. Flash photolysis in human cones. *Photochem Photobiol.* 1964;3:561–577.
9. Piñero D, Ortiz D, Alio J. Ocular scattering. *Optom Vis Sci.* 2010;87(9):E682–E696.
10. Ginis H, Perez G, Bueno J, Pennos A, Artal P. Wavelength dependence of the ocular straylight. *Invest Ophthalmol Vis Sci.* 2013;54:3702–3708.
11. Jacques SL, Wang L. Monte Carlo modeling of light transport in tissues. In: Welch AJ, Van Gemert MJC, eds. *Optical-Thermal Response of Laser-Irradiated Tissue (Lasers, Photonics, and Electro-Optics)*. Boston, MA: Springer; 1995: 73–100.
12. Stamper DA, Lund DJ, Molchany JW, Stuck BE. Laboratory simulator and field pursuit tracking performance with females and males in the presence of laser glare. *Aviat Space Environ Med.* 1997;68(7):580–587.
13. Suter AH. *The Effects of Noise on Performance*. Aberdeen Proving Ground, MD: US Army Human Engineering Laboratory; 1989. Technical Memorandum 3-89. <http://www.dtic.mil/dtic/tr/fulltext/u2/a212519.pdf>. Accessed October 16, 2017.
14. Hackley S, Johnson L. Distinct early and late subcomponents of the photic blink reflex: response characteristics in patients with retrogeniculate lesions. *Psychophysiology.* 1996;33:239–251.
15. Matania A, Parikh S, Bryan C, et al. Intrinsically photosensitive retinal ganglion cells are the primary but not exclusive circuit for light aversion. *Exp Eye Res.* 2012;105:60–69.
16. Dolgonos S, Ayyala H, Evinger C. Light-induced trigeminal sensitization without central visual pathways: another mechanism for photophobia. *Invest Ophthalmol Vis Sci.* 2011;52(11):7852–7858.
17. Baljet B, VanderWerf F. Connections between the lacrimal gland and sensory trigeminal neurons: a WGA/HRP study in the cynomolgous monkey. *J Anat.* 2005;206(3):257–263.
18. Duke-Elder S. *System of Ophthalmology: The Physiology of the Eye and of Vision*. Vol 4. St. Louis, MO: Mosby; 1968.
19. Shirzad-Wasei N, DeGrip W. Heterologous expression of melanopsin: present, problems and prospects. *Prog Retinal Eye Res.* 2016;52:1–21.
20. Neuman S, Haverkamp S, Auferkorte O. Intrinsically photosensitive ganglion cells of the primate retina express distinct combinations of inhibitory neurotransmitter receptor. *Neuroscience.* 2011;199:24–31.
21. Bailes HJ, Lucas RJ. Human melanopsin forms a pigment maximally sensitive to blue light ( $\lambda_{max} \approx 479$  nm) supporting activation of Gq/11 and Gi/o signalling cascades. *Proc Biol Sci.* 2013;280(1759):20122987.
22. Dacey DM, Liao HW, Peterson BB, et al. Melanopsin-expressing ganglion cells in primate retina signal colour and irradiance and project to the LGN. *Nature.* 2005;433:749–754.
23. Rushton W, Powell D. The rhodopsin content and the visual threshold of human rods. *Vis Res.* 1971;12:1073–1081.

24. Stuck BE. The blink and the blink reflex. Bioeffects Data, Supplement 1. Classified, Unclassified. In: Beatrice ES, Penetar DM, eds. *Handbook of Laser Bioeffects Assessment, Volume 1*. Presidio of San Francisco, CA: Letterman Army Institute of Research; 1984: S23–S28. Classified, Secret.
25. Reidenbach H-D, Hofmann J, Dollinger K, Seckler M. A critical consideration of the blink reflex as a means for laser safety regulations. In: Proceedings of the 11th International Congress of the International Radiation Protection Association. May 23–28, 2004; Madrid, Spain. <http://irpa11.irpa.net/pdfs/8c5.pdf>. Accessed October 16, 2017.
26. Reidenbach H-D, Hofmann J, Dollinger K. Active physiological protective reactions should be used as a prudent precaution safety means in the application of low-power laser radiation. *IFMBE Proceedings*. 2006;14:1,2690–2693.
27. Gerathewohl, S, Strughold H. Motoric responses of the eyes when exposed to light flashes of high intensities and short duration. *Aviat Med*. 1953;24:200–207.
28. Stamper DA, Lund DJ, Molchany JW, Stuck BE. Binocular and monocular laser glare effects on eye blink and tracking performance. Paper presented at: 25th Annual Lasers on the Modern Battlefield Conference; February 2004; Brooks City-Base, TX.
29. Glickman R. Differential effects of short- and long-pulsewidth laser exposures on retinal ganglion cell response. *Lasers Surg Med*. 1987;7:434–440.
30. Burke J, Hackley S. Prepulse effects on the photic eye blink reflex: evidence for startle-dazzle theory. *Psychophysiology*. 1997;34:276–284.
31. Laeng B, Endestad T. Bright illusions reduce the eye's pupil. *Proc Natl Acad Sci USA*. 2012;109(6):2162–2167.
32. Plainis S, Murray I, Carden D. The dazzle reflex: electrophysiological signals from ocular muscles reveal strong binocular summation effects. *Ophthalmic Physiol Opt*. 2006;26:318–325.
33. Ness J, Zwick H, Stuck B, et al. Retinal image motion during deliberate fixation: Implications to laser safety for long duration viewing. *Health Phys*. 2000;78:131–142.
34. Stiles WS, Crawford BH. The luminous efficiency of rays entering the eye pupil at different points. *Proc R Soc Lond B*. 1933;112(778):428–450.
35. Zwick H, Ness J, Molchany J, Stuck BE, Loveday J. Neural motor ocular strategies associated with the development of a pseudofovea following laser induced macular damage and artificial macular occlusion. Is the fovea replaceable? *J Laser Applications*. 1998;10:144–147.
36. Zwick H, Ness J, Molchany J, Stuck BE. Comparison of artificial and accidental laser-induced macular scotomas on human contrast sensitivity. In: Belkin M, Stuck BE, eds. *Laser-Inflicted Eye Injuries: Epidemiology, Prevention and Treatment*. *Proc SPIE*. 1996;2674:136–143.
37. Navarro R. The optical design of the human eye: a critical review. *J Optom*. 2009;2(1):3–18. doi: 10.3921/joptom.2009.3.
38. Stamper D, Lund D, Molchany J, Stuck B. Laser-induced afterimages in humans. *Percept Motor Skills*. 2000;91:15–33.
39. Geisler W. Initial-image and afterimage discrimination in the human rod and cone systems. *J Physiol*. 1979;294:165–179.
40. Geisler W. Adaptation, afterimages and cone saturation. *Vis Res*. 1977;18:279–289.
41. O'Mara PA, Stamper DA, Beatrice ES, et al. *BLASER: A Simulator for the Investigation of Biomedical Factors Influencing Laser Designator Operator Performance*. Presidio of San Francisco, CA: Letterman Army Institute of Research; 1979. Technical Note No. 79–10TN.
42. Stamper DA, Lund DJ, Molchany JW, Stuck BE. Transient disruption of human pursuit tracking performance for laser exposures below permissible exposure limits. In: Stuck BE, Belkin M, eds. *Lasers and Noncoherent Ocular Effects: Epidemiology, Prevention and Treatment*. *Proc SPIE*. 1997;2974:117–128.

43. Stamper DA, Levine RR, Best PR. Effect of practice schedule on two-hand pursuit tracking performance. *Percept Motor Skills*. 1987;65:483–492.
44. Levine RR, Lund DJ, Stuck BE, Stamper DA, Beatrice ES. *Project Morningstar: Effects of Glare Produced by Low-Level Helium-Neon (632.8 nm) Laser Radiation on Human Pursuit Tracking Performance*. Presidio of San Francisco, CA: Letterman Army Institute of Research; 1985. Institute Report No. 203.
45. Stamper D, Lund D, Molchany J, Dembrowsky, Boneta O, Stuck B. *Validation of the Blaser II Laboratory Tracking System*. Silver Spring, MD: Walter Reed Army Institute of Research; 1997. Technology Report 97–001.
46. American National Standards Institute. *American National Standard for Safe Use of Lasers: ANSI Z136.1-2000*. Orlando, FL: Laser Institute of America; 2007.
47. Lund B, Zwick H, Lund D, Stuck B. Effect of source intensity on ability to fixate: implications for laser safety. *Health Phys*. 2003;85(5):567–577.
48. Ponder E, Kennedy WP. On the act of blinking. *Q J Exp Phys*. 1927;18:89–110.
49. Alpern M, Holland M, Ohba N. Rhodopsin bleaching signals in essential night blindness. *J Physiol*. 1972;225:457–476.
50. Curcio C, Allen K. Topography of ganglion cells in human retina. *J Comp Neurol*. 1990;300(1):5–25.
51. Abrams R, Meyer D, Kornblum S. Speed and accuracy of saccadic eye-movements: characteristics of impulse variability in the oculomotor system. *J Exp Psychol Hum Percept Perform*. 1989;15(3):529–543.
52. Stamper D, Lund D, Molchany J, Stuck B. Human pupil and eyelid response to intense laser light: implications for protection. *Percept Motor Skills*. 2002;95:775–782.
53. Ness JW, Zwick H, Molchany JW. Preferred retinal location induced by macular occlusion in a target recognition task. In: Belkin M, Stuck BE, eds. *Laser-Inflicted Eye Injuries: Epidemiology, Prevention and Treatment*. *Proc SPIE*. 1996;2674:131–135.
54. Barlow H, Fitzhugh R, Kuffler S. Change of organization in the receptive fields of cat's retina during dark adaptation. *J Physiol*. 1957;137:338–354.
55. Brindley G. Two new properties of foveal afterimages and a photochemical hypothesis to explain them. *J Physiol*. 1962;164:168–179.
56. Crane CC. Phase IV operations: where wars are really won. *Milit Rev*. 2005;85(3):27–36.